Journal of Solid State Chemistry **163,** 340–349 (2002)
doi:10.1006/jssc.2001.9428, available online at http://www.idealibrary.com on IDEAL®

Structural and Thermal Characteristics of Nickel Dioxide Derived from $LiNiO_2$

Hajime Arai,[1] Masayuki Tsuda, Keiichi Saito, Masahiko Hayashi, Koji Takei, and Yoji Sakurai

NTT Telecommunications Energy Laboratories, NTT Corporation

Received July 31, 2001; accepted October 5, 2001

We report the structural and thermal characteristics of highly delithiated (lithium extracted) compounds Li_xNiO_2, which can be called "nickel dioxide." We obtained $Li_{0.10}NiO_2$ and $Li_{0.04}NiO_2$ by treating $LiNiO_2$ with sulfuric acid. Both products contained phases with NiO_2 stacking similar to cadmium chloride (O3-type), but the latter also included a phase with NiO_2 stacking similar to cadmium iodide (O1-type). We examined their thermal behavior using high temperature X-ray diffraction analysis together with thermogravimetric analysis and found that novel polymorphs, with similar chemical compositions but different structures, were obtained by heating them at appropriate temperatures. We discuss these results together with those for Li_xNiO_2 obtained by electrochemical delithiation. We also report acid-treated products derived from $Li_{0.93}Ni_{1.07}O_2$. © 2002 Elsevier Science

Key Words: **nickel dioxide; lithium nickelate; chemical delithiation; acid treatment; thermal characteristics; soft chemistry; electrochemistry; electrodes.**

1. INTRODUCTION

The usual oxidation state of nickel is $+2$ and only a limited number of compounds have Ni^{3+} or Ni^{4+}, other than complexes with organic-ligands (1). Oxides and halides with Ni^{4+} are particularly rare. Only a few compounds such as K_2NiF_6, $BaNiO_3$, and $KNiIO_6$ have been identified while the existence of "NiO_2 (nickel dioxide)" had been thought doubtful (1). In contrast, lithium nickelate $LiNiO_2$ is widely studied as an active electrode material for lithium batteries. $LiNiO_2$ definitely contains Ni^{3+} and has a very large capacity. This means that lithium can be electrochemically extracted from $LiNiO_2$ to form Li_xNiO_2, leading to the formation of species containing Ni^{4+}. The structure of Li_xNiO_2 has also been studied, showing it to have a well-defined layered crystal structure similar to that of pristine $LiNiO_2$. At $x \leq 0.3$, several research groups have found a phase with Ni–O distances much shorter than those of $LiNiO_2$ (2–6) and concluded that this indicated the formation of Ni^{4+}–O^{2-} bonds. It has recently been reported by two research groups that, in a highly delithiated (lithium-extracted) state corresponding to $x \approx 0$ in Li_xNiO_2 (considered to be "nickel dioxide"), the pristine cubic close-packed oxygen arrangement (denoted as "O3") changes into the hexagonal close-packed structure (denoted as "O1") to form NiO_2 with a cadmium iodide structure (7–12), which is isostructural with completely delithiated lithium cobaltate Li_xCoO_2 with $x \approx 0$ (5).

In contrast to electrochemical delithiation, chemical delithiation offers the advantage of being free from conductive agents and/or electrode binders; it is thus suitable for evaluating the intrinsic characteristics of delithiated materials. Acid treatment (or acid leaching) is a useful delithiation method (13) and has been used for chemical delithiation from nonstoichometric lithium nickelate $Li_{1-x}Ni_{1+x}O_2$ (14–17), as well as chemical oxidation using a strong oxidizer (18). In our previous study we employed this acid treatment for delithiating from stoichiometric $LiNiO_2$ to prepare Li_xNiO_2 with various x values (19, 20). Our recent preliminary study has indicated that, under certain specific conditions, the NiO_2 phase with a cadmium iodide structure is also obtained by acid treatment (21).

In this, study we focus on highly delithiated Li_xNiO_2 prepared by acid treatment and report its synthesis, structure and thermal behavior. In particular we detail two compounds that can be called nickel dioxide, $Li_{0.10}NiO_2$ and $Li_{0.04}NiO_2$, which were obtained using concentrated sulfuric acid treatment. The structure was examined using X-ray diffraction (XRD) patterns together with the Rietveld analysis. The high oxidation state was analyzed by iodometry and X-ray photoelectron spectroscopy (XPS). We examined the thermal stability of the highly delithiated phases using high-temperature XRD measurement and thermogravimetry (TG) combined with differential scanning calorimetry (DSC). Using the advantage of having chemically obtained samples, we isolated and characterized several high-temperature phases of Li_xNiO_2. We also describe

[1]To whom correspondence should be addressed. E-mail: arai@iba.iecl.ntt.co.jp.

0022-4596/02 $35.00

the results that were obtained when nonstoichiometric $Li_{1-x}Ni_{1+x}O_2$ was used as the starting material.

2. EXPERIMENTAL

We synthesized stoichiometric $LiNiO_2$ with a nearly complete layered structure as previously reported (4). Nonstoichiometric lithium nickelate $Li_{0.93}Ni_{1.07}O_2$ was obtained by heating a mixture of $LiOH \cdot H_2O$ and $Ni(OH)_2$ in a molar ratio of 1 : 1 at 700°C for 24 h. The $LiNiO_2$ exhibited lattice parameters of $a = 2.875$ Å and $c = 14.193$ Å while those of $Li_{0.93}Ni_{1.07}O_2$ were $a = 2.882$ Å and $c = 14.203$ Å, respectively. A detailed structural and electrochemical characterization of these samples has already been published (4, 6).

The acid leaching process was carried out by adding the nickelate compound to an aqueous solution of sulfuric acid. The mixture was stirred at 25°C for 5 h unless otherwise specified. The initial molar ratio of $H^+/LiNiO_2$ was 5, indicating that a sufficient quantity of acid was supplied for the completion of the following disproportionation reaction of nickel ($2Ni^{3+} \rightarrow Ni^{4+} + Ni^{2+}$).

$$LiNiO_2 + 4yH^+ \rightarrow (1-y)Li_{(1-2y)/(1-y)}NiO_2 + yNi^{2+} + 2yLi^+ + 2yH_2O \ (0 \le y \le 0.5) \quad [1]$$

We used filtration to extract a grayish powder from the green solution containing Ni^{2+}. This powder was washed with acetone to remove the water on its surface and dried in a vacuum at room temperature.

The chemical composition of the product was evaluated using inductively coupled plasma emission (ICPE) spectroscopy to analyze lithium and nickel. The nickel oxidation state was analyzed using iodometry. We also employed XPS to evaluate the oxidation state, using Mg$K\alpha$ radiation (ESCA 5400, ULVAC-PHI, Inc.). The binding energy values were referenced to the carbon 1s line that was taken as 284.0 ± 0.3 eV. We used a neutralizer to eliminate the influence of the sample charge-up.

The crystal structure was analyzed using XRD analysis with Cu$K\alpha$ radiation (Rigaku RAD-RX and RINT 2500HF). The diffraction intensity was measured stepwise in 0.02° steps for diffraction angles 2θ between 15° and 85°. We performed the Rietveld analysis with the aid of the computer program RIETAN (22, 23). The obtained agreement factor R_{wp} (24) was typically 10–15. For the high temperature XRD measurements we set the temperature at 20°C intervals from 100 to 300°C, and scanned the diffraction angle 2θ between 15° and 50° at a constant scanning speed of 5° min^{-1}. The temperature was maintained for 5 min prior to the XRD measurement.

We measured the thermal behavior using TG-DSC (Rigaku TAS-100). The sample was heated to 700°C in an argon atmosphere at a heating rate of 10°C min^{-1}.

We also examined electrochemical delithiation from $LiNiO_2$ using coin cells (4) with metallic lithium as the counter (negative) electrode. The working (positive) electrode mixture consisted of nickelate powder (70 wt%), acetylene black (25 wt%) and polytetrafluoroethylene (5 wt%). The electrolyte was a 1 mol dm^{-3} $LiPF_6$ solution in equal volumes of ethylene carbonate and dimethyl carbonate. The delithiation process was conducted at a constant current density of 0.1 mA cm^{-2} until the cell voltage reached 4.5 V. The cell temperature was set at 20 or 40°C. We calculated the lithium content of the electrode from the weight of the electrode and the transferred charge.

3. RESULTS AND DISCUSSION

3.1. Structure of Acid-Treated Products

In our preliminary study we found that sulfuric acid was most effective for obtaining highly delithiated nickelate compounds (20). When we used acid solutions at the same concentration, the degree of delithiation was in the following order; sulfuric acid > hydrochloric acid > phosphoric acid ≈ nitric acid ≫ acetic acid. In this study we changed the sulfuric acid concentration and examined the effect on the structure of the delithiated compounds. Figure 1 shows the XRD patterns of the delithiated compounds that we obtained by treating $LiNiO_2$ with sulfuric acid at various concentrations for 5 h. As shown, all the delithiated samples had XRD patterns similar to that of $LiNiO_2$, suggesting that the pristine layered structure was essentially maintained. However, as the acid concentration became higher, several additional peaks appeared, for instance at $2\theta = 42.5°$ and $2\theta = 56.5°$, indicating that a new phase had emerged. We chose the patterns shown in Figs. 1c and 1f and conducted

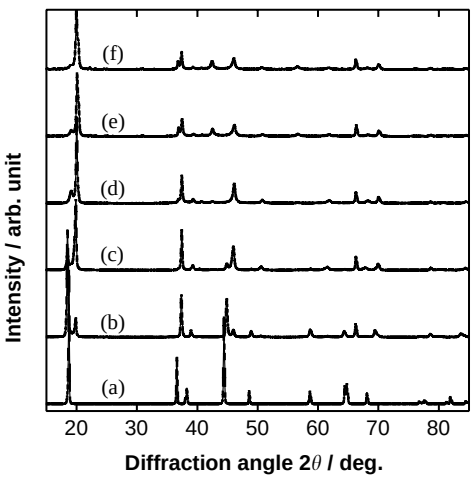

FIG. 1. XRD patterns of (a) $LiNiO_2$ and its delithiated products treated with (b) 0.4, (c) 0.6, (d) 0.9, (e) 1.2, and (f) 1.8 mol dm^{-3} sulfuric acid solutions for 5 h.

detailed analyses. We denote these compounds that were treated with 0.6 and 1.8 mol dm^{-3} acid solutions as samples A and B, respectively.

Sample A had an Li/Ni value of 0.10, as indicated by ICPE spectroscopy. The XRD pattern shown in Fig. 1c is similar to that of $Li_{0.10}NiO_2$ prepared by electrochemical delithiation (4). Thus we applied the structural model of the electrochemically obtained $Li_{0.10}NiO_2$, and successfully analyzed the XRD pattern. Sample A consisted of two phases, each of which had an element configuration of $[Li_x]_{3b}[Ni]_{3a}[O_2]_{6c}$ with a space group of $R\bar{3}m$. Table 1 lists the structural parameters of sample A. The calculated Ni–O distances for both phases accord well with the sum of the ionic radii of Ni^{4+} (low spin) and O^{2-} of 1.88 Å (25). In addition to the parameters listed in Table 1, the Rietveld analysis indicated that there are neither nickel atoms in the lithium (3b) layer nor oxygen vacancies in the material. The iodometry showed that the oxidation state of nickel was 3.8 ± 0.1. By taking the experimental error into consideration, we concluded that there was no oxygen vacancy in the material. A proton exchange reaction with lithium was unlikely because the possible product β-NiOOH was not detected by XRD analysis. The surface water/proton content also seemed low because sample A showed no weight change up to 190°C, as described later. Although the XRD analysis gave little information on the lithium content in each phase due to the small scattering factor of lithium, we suggest that phase A1 corresponds to the lithium-rich phase because the phase with a c parameter of less than 13.6 Å is observed only when x in Li_xNiO_2 is close to zero (2–6).

In addition to the iodometry, we performed an XPS study to examine the oxidation state of nickel contained in sample A ($Li_{0.10}NiO_2$). We measured the spectra of Ni, NiO, $LiNiO_2$, and sample A, and compared the binding energy of Ni $2p_{3/2}$, as listed in Table 2. There is a general trend that the binding energy increases as the oxidation state increases, although there are some discrepancies in the values reported in the references. As the differences between Ni(III) and Ni(IV) are small on the energy level, it is difficult to assign the observed peak to a particular state. Nevertheless, it is at least clear that $LiNiO_2$ and sample A consist of Ni(III) and/or Ni(IV).

Sample B treated with the 1.8 mol dm^{-3} solution had an Li/Ni value of 0.04, showing its high degree of delithiation. As mentioned above, sample B exhibited several additional peaks in the XRD profile in addition to those observed in sample A, suggesting that a new phase was formed. Our preliminary study has shown that this phase can be characterized as an NiO_2 phase with a cadmium iodide structure (21). We therefore assumed that this additional phase belongs to the space group of $P\bar{3}m1$ with an element configuration of $[Ni]_{1a}[O_2]_{2d}$. Figure 2 shows the result of the Rietveld analysis. The experimental and calculated patterns were nearly identical, and the peaks were fully indexed.

TABLE 1
Treatment Conditions, Chemical Compositions, and Structural Parameters of Nickelate Samples

Sample	Starting material	Treatment condition	Li/Ni ratio[b]	Phase name	Weight ratio (%)	Space group	a/Å[c]	c/Å[c]	u(O)	Ni–O distance/Å
A	$LiNiO_2$	0.6 mol dm^{-3} sulfuric acid[a]	0.10	A1	18	$R\bar{3}m$	2.8152(8)	14.357(4)	0.268(9)[d]	1.877
				A2	82	$R\bar{3}m$	2.8180(3)	13.411(2)	0.265(4)[d]	1.867
B	$LiNiO_2$	1.8 mol dm^{-3} sulfuric acid [a]	0.04	B1	6	$R\bar{3}m$	2.817(2)	13.82(1)	0.27(2)d[d]	1.85
				B2	73	$R\bar{3}m$	2.819(1)	13.318(3)	0.269(1)[d]	1.846
				B3	21	$P\bar{3}m1$	2.818(2)	4.367(2)	0.209(8)[e]	1.87
C	$Li_{0.93}Ni_{1.07}O_2$	0.6 mol dm^{-3} sulfuric acid[a]	—	C1	100	$R\bar{3}m$	2.8241(1)	14.353(1)	0.265(2)[d]	1.903
D	$Li_{0.93}Ni_{1.07}O_2$	1.8 mol dm^{-3} sulfuric acid[a]	—	D1	100	$R\bar{3}m$	2.8236(3)	14.038(2)	0.266(4)[d]	1.884
E	Sample A	Heated at 160°C for 15 h	(0.10)	A3	100	$R\bar{3}m$	2.834(2)	14.36(1)	0.26(3)[d]	1.87
F	Sample E	Heated at 170°C for 6 h	(0.10)	A4	100	$Fd\bar{3}m$	8.102(1)	—	0.390(3)[f]	1.91
G	Sample B	Heated at 180°C for 1 h	(0.04)	B4	100	$R\bar{3}m$ (?)	2.92 (2)	14.2(1)	0.27(1)[d]	1.9

[a] Delithiation using specified acid solution for 5 h.
[b] Measured by ICPE spectroscopy
[c] Lattice parameters in a hexagonal setting except for sample F in a cubic setting.
[d] Positions of lithium, nickel, and oxygen in $3b$ $(0, 0, \frac{1}{2})$, $3a$ $(0, 0, 0)$, and $6c$ $(0, 0, u)$ sites, respectively.
[e] Positions of nickel and oxygen in $1a$ $(0, 0, 0)$ and $2d$ $(\frac{1}{3}, \frac{2}{3}, u)$ sites, respectively.
[f] Positions of lithium, nickel, and oxygen in $8a$ $(0, 0, 0)$, $16d$ $(\frac{5}{8}, \frac{5}{8}, \frac{5}{8})$ and $32e$ (u, u, u) sites, respectively.

TABLE 2
Binding Energy of Ni $2p_{3/2}$ in eV, Obtained by XPS Study

Reference	Ni (0)	Ni (II)	Ni(III)	Ni(IV)
This study	Ni, 852.3	NiO, 854.2	$LiNiO_2$, 854.8	$Li_{0.10}NiO_2$, 855.1
[26–28]		NiO, 854.1	NiOOH, 855.3	$KNiIO_6$, 855.4
[29]		$Ni(OH)_2$, 853.4	$LiNiO_2$, 856.0	
[30]	Ni, 852.3	NiO, 854.1	NiOOH, 856.7	

Figure 2 includes the indices of certain distinct peaks of the phase with a cadmium iodide structure.

Table 1 lists the structural parameters of the three phases contained in sample B. The Rietveld analysis indicated that none of the phases in sample B contained oxygen vacancies or nickel atoms in the lithium layer. All the phases exhibited calculated Ni–O distances of about 1.85 Å, which are again close to the sum of the ionic radii of Ni^{4+} (low spin) and O^{2-} of 1.88 Å (25). Phase B3 is isostructural with β-NiOOH, nevertheless, the lattice parameter c (4.37 Å) is much shorter than that of β-NiOOH (4.81 Å), suggesting that phase B3 is proton-free.

The simultaneous coexistence of three phases is thermodynamically unfavorable. This means that one of the three phases is only kinetically stable (metastable) and is being transformed to a thermodynamically more stable phase. Figure 3 provides schematic views of phases B1, B2, and B3. Most of the lithium is presumably incorporated in phase B1 because this phase has the longest interlayer distance as does phase A1. The NiO_2 units in phases B1 and B2 have stacking arrangements similar to cadmium chloride with a cubic close-packed structure (O3 type), while those in phase B3 resemble cadmium iodide with a hexagonal close-packed structure (O1 type). Note that three times the c value in phase B3 is close to the c value in phase B2 (also see Table 1). Taking the similarity between phases B2 and B3 into account, we concluded that phase B2 was partly transformed into phase B3 as a result of two thirds of the NiO_2 layers in phase B2 sliding. As such sliding (or gliding) is feasible when the lithium layer is empty, we believe that phase B1 is the phase incorporating most of the lithium.

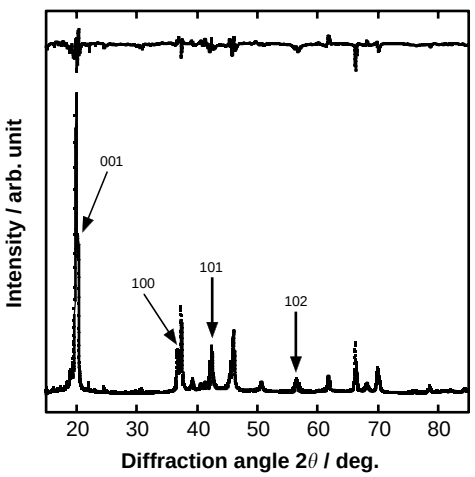

FIG. 2. Result of Rietveld analysis of sample B. The upper part of the figure shows the difference between experimental and calculated intensity. Some indices for phase B3 are also shown.

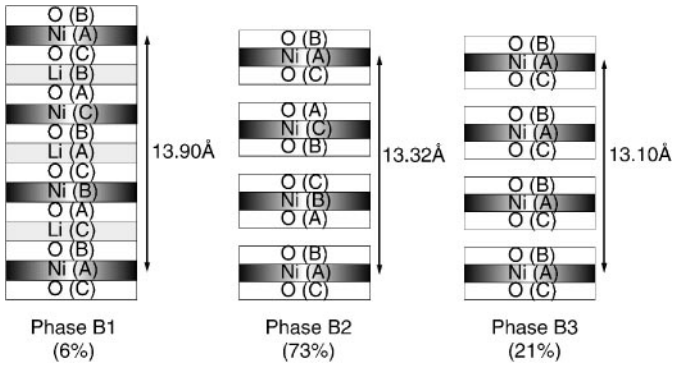

FIG. 3. Schematic views of phases B1, B2, and B3. The layer distances, corresponding to c in phases B1 and B2 and $3c$ in phase B3, are shown. (A), (B), and (C) are stacking configurations.

The highly delithiated phases we obtained in this study are nearly identical to those reported by Croguennec *et al.* (9–12), who obtained Li_xNiO_2 by electrochemical delithiation with continuous charging. Our phases A1 and A2 correspond to their phases R2 and R3 while our phases B1, B2, and B3 involved in the more delithiated nickelate accord with their phases R2′, R3′, H4, respectively. The structural parameters are also similar, indicating that our chemical delithiation process leads to results almost the same as those obtained with electrochemical charging. Seguin, Tarascon, and their coworkers have also obtained the NiO_2 phase with a cadmium iodide structure using electrochemical delithiation (7, 8) and have suggested that the phase belongs to a monoclinic system, which is inconsistent with our result for phase B3. The two Ni–O distances of 1.922 and 1.952 Å, calculated from their structural data, are different from ours (1.87 Å), and seem too long to be Ni(IV)–O distances. This discrepancy may be because their starting $LiNiO_2$, with $a = 2.862$ Å and $c = 14.113$ Å, is very different from ours with $a = 2.875$ Å and $c = 14.193$ Å. The structure of CoO_2 has recently been re-examined to prove that CoO_2 contains two phases with the cadmium iodide structure ($a = 2.805$ with $c = 4.251$ Å and $a = 2.821$ with $c = 4.240$ Å) (8). Recently reported $Li_xNi_{0.8}Co_{0.2}O_2$ with $x \approx 0$ also shows a structure similar to our phase B3, with $a = 2.814$ and $c = 4.590$ Å (31).

In our previous study, we were unable to detect phase B3 by constant current electrochemical charging (4, 6). Figure 4 a depicts the XRD pattern of $Li_{0.04}NiO_2$ obtained by electrochemical delithiation at 20°C, showing that the peak

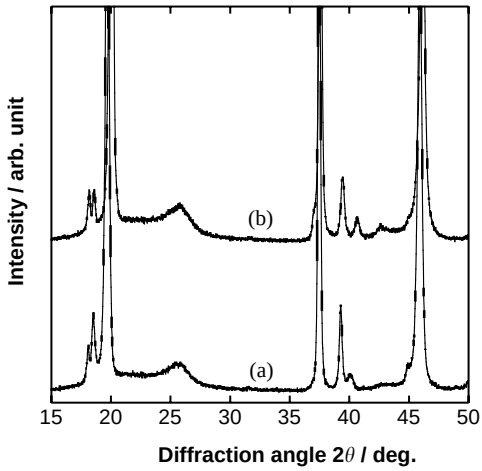

FIG. 4. XRD patterns of $Li_{0.04}NiO_2$ delithiated electrochemically with cell temperature at (a) 20°C and (b) 40°C. The charging current density was 0.1 mA cm^{-2} and the final QOCV was 4.25 V. The sharp peak at 18° and broad peak at 26° belong to polytetrafluoroethylene (binder) and acetylene black (conductive agent), respectively.

at $2\theta = 42.5°$, the indicator for phase B3, was very weak. However, when we raised the cell temperature to 40°C, the product $Li_{0.04}NiO_2$ showed a distinct peak at $2\theta = 42.5°$, as shown in Fig. 4 b. We believe this is because the formation was kinetically accelerated at the elevated temperature.

Figure 5 summarizes the c and $3c$ values for the phases with space groups of $R\bar{3}m$ (phases A1, A2, B1, and B2) and $P\bar{3}m1$ (phase B), respectively, obtained under various conditions. The weight ratio of each phase is indicated in parentheses. The sample we prepared with the 1.8 mol dm^{-3} solution additionally contained $NiSO_4 \cdot 2H_2O$ (Joint Committee on Powder Diffraction Standards 17-483) as a very minor impurity, but we disregarded this in the weight ratio calculation. Figure 5 shows that, as the acid concentration increases, the weight ratio of the lithiated phases A1 and B1 becomes lower and that of phase B3 higher. The figure also shows that the lattice parameters change greatly when the acid concentration exceeds a certain value (≈ 0.8 mol dm^{-3}). This can be related to the x value in each Li_xNiO_2 sample, but further study is required to understand the phenomenon.

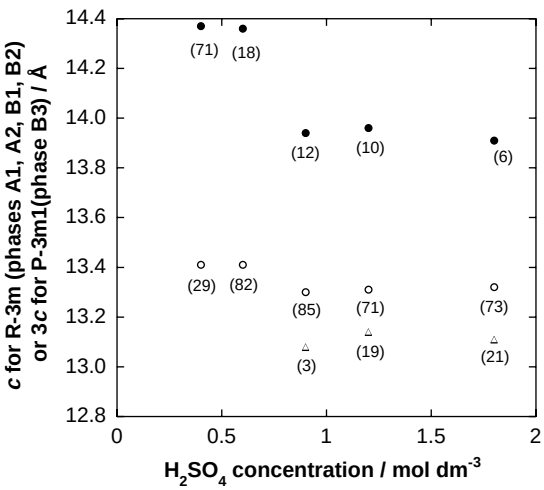

FIG. 5. Layer distances c and $3c$ for phases with space groups of $R\bar{3}m$ (phases A1 and B1 with filled circles, phases A2 and B2 with open circles) and $P\bar{3}m1$ (phase B3 with open triangles), respectively, obtained under various conditions. The number in the parentheses corresponds to the weight ratio of each phase.

Reaction [1] allows us to estimate the yield of the acid treatment, i.e., the weight ratio of the solid nickelate residue to the starting $LiNiO_2$. The yield will be 46% when the disproportionation reaction of nickel is complete and half the nickel atoms in $LiNiO_2$ dissolve in the acid solution.

$$LiNiO_2 + 2H^+ \rightarrow 0.5\ NiO_2 + 0.5\ Ni^{2+} + Li^+ + H_2O \quad [2]$$

Interestingly, the yield was a good indicator with which to estimate the structural nature of the acid-treated product. When the product contained two phases similar to sample A, the yield was larger than 46%. The yield was lower (typically 30–45%) when the product was similar to sample B with a cadmium iodide structure. Such a low yield indicates that the "NiO_2" phase was also dissolved in acid solutions, since there was an excess of protons under our experimental conditions, even after reaction [2] had finished. Thus, a longer treatment time resulted in further dissolution and/or delithiation of the product. For example, the acid treatment with a 0.4 mol dm^{-3} solution for 5 h, shown in Fig. 1b, led to a product nearly identical to that obtained by treatment with a 0.6 mol dm^{-3} solution for 3 h. Unlike the acidic media, products such as sample A were stable in neutral water or in a dry atmosphere, at room temperature for at least several weeks.

We also examined chemical delithiation from $Li_{0.93}Ni_{1.07}O_2$. This material had an element configuration of $[Li_{0.93}Ni_{0.07}]_{3b}[Ni]_{3a}[O_2]_{6c}$, namely, it contained a considerable amount of nickel in the lithium predominant layer. The acid-treated product always consisted of a single phase with a similar structure to the pristine material, and we obtained no phase with the cadmium iodide structure, even when we used concentrated acid solution for the treatment, as shown in Fig. 6 and Table 1. This is because the nickel atoms in the lithium layer prevent the layer from sliding, and so prevent the formation of the NiO_2 phase with the cadmium iodide structure. Previous reports on chemical (14–18) and electrochemical delithiation (10) have also revealed that highly delithiated states, even those corresponding to sample A, are hardly obtained with nonstoichiometric lithium nickelate. Nevertheless, the calculated Ni–O distan-

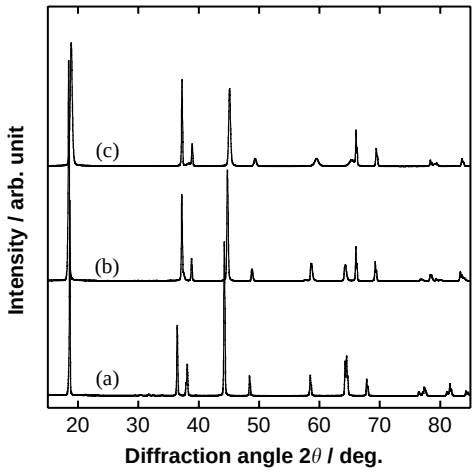

FIG. 6. XRD patterns of (a) $Li_{0.93}Ni_{1.07}O_2$ and its delithiated products treated with (b) 0.6 and (c) 1.8 mol dm^{-3} sulfuric acid solutions for 5 h.

ces for samples C and D were again close to the sum of the ionic radii of Ni^{4+} (low spin) and O^{2-} of 1.88 Å (25), indicating that the nickel contained in these samples was largely Ni^{4+}. The fact that sample D has shorter lattice parameters than sample C indicates the high degree of delithiation under strongly acidic conditions.

3.2. *Thermal Behavior of Li_xNiO_2*

The thermal behavior of Li_xNiO_2 electrodes has been of great interest because it affects battery safety (32–37). When x is close to zero, the material contains a large amount of metastable Ni^{4+} and decomposes exothermically at elevated temperatures. We have used TG-DSC to prove that Li_xNiO_2 decomposes according to the following reaction to form a nickelate product with a rocksalt structure ($Li_{1-z}Ni_zO$) and gaseous oxygen (20).

$$Li_xNiO_2 \rightarrow (1 + x)Li_{x/(1+x)}Ni_{1/(1+x)}O + (1 - x)/2O_2. \quad [3]$$

Although the final product with the rocksalt phase has been clarified, there has been little information on the detailed structural changes that occur until reaction [3] has finished. On this basis we examined the thermal behavior of samples A and B using high-temperature XRD and TG-DSC measurements. Using the advantage of chemical delithiation, we were able to isolate novel kinds of heat-treated Li_xNiO_2, as described below.

Figure 7 shows the XRD patterns of sample A heated at temperatures between room temperature and 300°C. The pattern was unchanged until the temperature reached 100°C. At 120°C a new peak appeared at $2\theta \approx 19°$ that was similar to the peak of phase B1, and simultaneously the peak at $2\theta \approx 20°$ for phase A2 began to decrease. This instability of phase A2 agrees with a previously reported result (36). At 180°C these peaks were almost unified into a single peak, suggesting that a single phase was formed. At 200°C new peaks appeared at $2\theta \approx 31°$, 36.5°, and 38°, suggesting that a new phase had emerged. This XRD pattern is similar to that of spinel $LiNi_2O_4$, which is obtained by heating layered $Li_{0.5}NiO_2$ at around 200°C (14, 15, 18, 38, 39). This spinel phase presumably had nickel atoms in the originally lithium (8*a*) sites, because the 220 diffraction intensity would be very small if the 8*a* sites are exclusively occupied by lithium. At 300°C, the peak at $2\theta \approx 18.5°$ weakened and the peaks at $2\theta \approx 37.5°$ and $2\theta \approx 44°$ enlarged, indicating that the rocksalt $Li_{1-z}Ni_zO$ phase became prominent.

According to the TG-DSC result shown in Fig. 8, the exothermic behavior began at around 180°C while the weight loss, corresponding to oxygen evolution (32), started at around 190°C. Taking these results into account, we

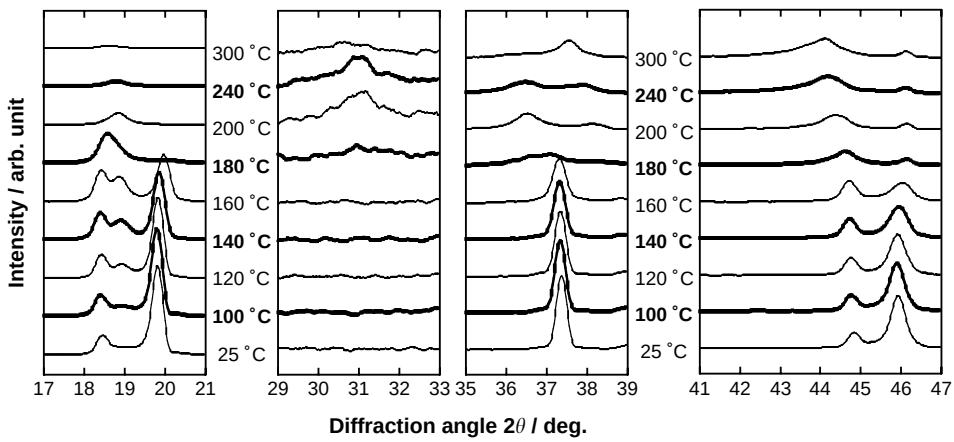

FIG. 7. XRD patterns of sample A heated at temperatures between 25 and 300°C. The intensity was varied for different angle regions for clarity. The peak at 46.2° corresponds to the 200 peak of platinum used as the sample holder.

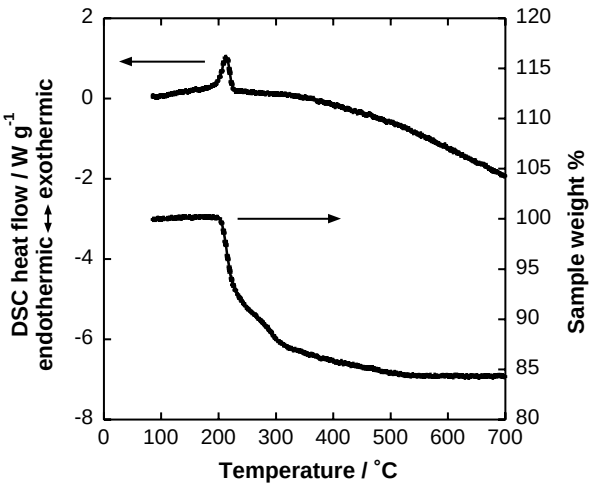

FIG. 8. TG-DSC profiles of sample A in an argon flow with a heating rate of 10°C min^{-1}.

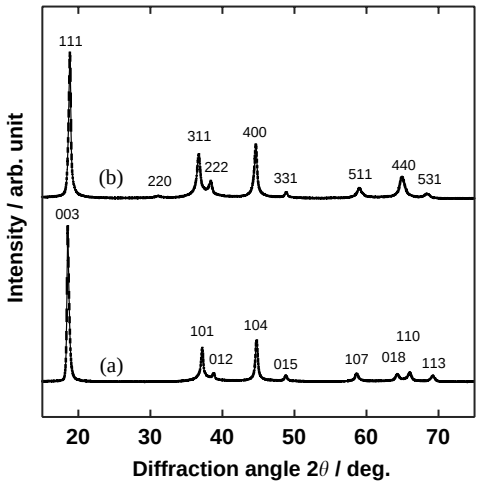

FIG. 9. XRD patterns of (a) sample E and (b) sample F, which were obtained by heating sample A at 160°C for 15 h and sample E at 170°C for 6 h, respectively. The indices in (a) and (b) are based on the space groups of *R*-3*m* and *Fd*-3*m*, respectively.

expected $Li_{0.10}NiO_2$ with a single phase at 180°C, in contrast to the pristine $Li_{0.10}NiO_2$ at room temperature with phases A1 and A2. Because we observed little heat flow when phases A1 and A2 (and partially B1) were transformed into this single phase, it seems that this change is only slightly favored energetically. The following formation of the disordered spinel phase must be much favored, because a considerable amount of exothermic heat was generated at 200°C. The exothermic heat was so large that we were unable to detect the endothermic heat generated by the oxygen evolution. The disordered spinel phase can be described as $Li_{0.2}Ni_2O_{4-\delta}$ because oxygen release has already started at this temperature, as suggested by the TG curve. There was no distinct DSC peak corresponding to the spinel–rocksalt transition, but it seemed that, as the temperature became high, the structure became highly disordered with releasing oxygen. The sample weight was nearly constant at temperatures above 500°C, and the final weight change at 700°C was 15.7%, which agrees well with the expected change of 15.8% in the following oxygen evolution reaction:

$$Li_{0.10}NiO_2 \rightarrow 1.1Li_{1/11}Ni_{10/11}O + 0.45O_2. \quad [4]$$

The final product had a rocksalt structure with a cubic lattice parameter of 8.35 (4.175 × 2) Å.

We tried to isolate novel phases with the nominal chemical composition of $Li_{0.10}NiO_2$ under appropriate conditions. We obtained a single-phase product (called sample E) with a space group of $R\bar{3}m$, by heating sample A at 160°C for 15 h. The new phase is denoted as phase A3. Although the change from phases A1 and A2 to phase A3 is only slightly favored, it turned out that this change is irreversible, namely, phase A3 remained after cooling from 160°C to room temperature. The yield was nearly unity, indicating that no oxygen was released. Figure 9a shows the XRD pattern. The peaks were well-defined, and we obtained the lattice parameters as shown in Tables 1 and 3. The c/a ratio of 5.07 is certainly larger than $\sqrt{24}$ (4.90), indicating that the cubic (spinel) system is inapplicable to phase A3. The Rietveld analysis suggested that the layered structure was maintained and that there were no nickel atoms in the lithium layer.

When we heated sample E further at 170°C for 6 h, the product (sample F) had a spinel structure, as shown in Fig. 9b. We denote this phase as phase A4. The yield was again nearly unity, indicating that this phase can also be described as "nickel dioxide." Tables 1 and 4 list the XRD data of sample F. We successfully indexed all the diffraction lines using the spinel structure with a space group of $Fd\bar{3}m$. The Rietveld analysis indicated that the spinel structure in

TABLE 3
XRD Data of $Li_{0.10}NiO_2$ Treated at 160°C for 15 h (Sample E)

h	*k*	*l*	d^a_{cal}/Å	d_{obs}/Å	I_{obs}
0	0	3	4.785	4.782	100
1	0	1	2.420	2.417	20
0	1	2	2.323	2.320	4
1	0	4	2.026	2.024	28
0	1	5	1.866	1.865	4
1	0	7	1.574	1.574	6
0	1	8	1.449	1.449	5
1	1	0	1.417	1.415	6
1	1	3	1.359	1.358	5

[a] $a = 2.834$ Å, $c = 14.36$ Å.

TABLE 4
XRD Data of $Li_{0.10}NiO_2$ Treated at 170°C for 6 h (Sample F)

h	k	l	d^a_{cal}/Å	d_{obs}/Å	I_{obs}
1	1	1	4.678	4.682	100
2	2	0	2.865	2.868	2
3	1	1	2.443	2.444	32
2	2	2	2.339	2.441	9
4	0	0	2.026	2.027	40
3	3	1	1.859	1.861	4
5	1	1	1.559	1.560	9
4	4	0	1.432	1.432	20
5	3	1	1.370	1.369	4

[a] $a = 8.102$ Å.

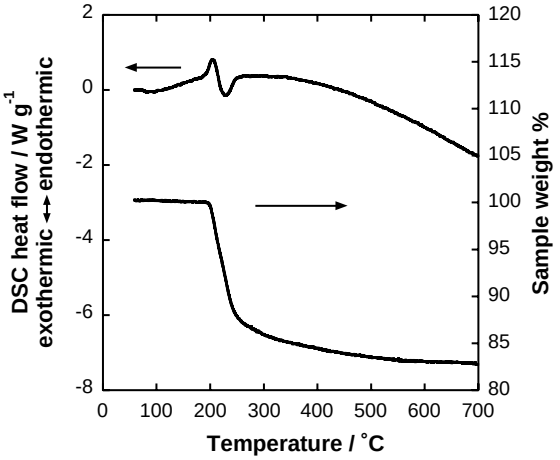

FIG. 11. TG-DSC profiles of sample B in an argon flow with a heating rate of 10°C min^{-1}.

phase A4 was mainly a normal type, but partly had an inverse nature with some nickel atoms in 8*a* sites. The obtained cubic lattice parameter (8.102 Å) is close to 8.08 Å for $LiNi_2O_4$ and 8.10 Å for $Li_{1.1}Ni_2O_4$ (39). When sample E was heated at 180°C, there was a weight loss due to oxygen evolution and the product had a disordered spinel structure with considerable nickel atoms in 8*a* and 16*c* sites. The obtained cubic lattice parameter was larger (e.g., 8.13 Å), due to the highly disordered nature of the sample.

We also examined the thermal behavior of sample B using high-temperature XRD and TG-DSC measurements. Figure 10 shows that, until the temperature reached 160°C, the peak at $2\theta \approx 42.5^\circ$ corresponding to phase B3 was nearly maintained while the peak at $2\theta \approx 20^\circ$ decreased. As both phases B2 and B3 have peaks at $2\theta \approx 20^\circ$, the above phenomenon indicates that phase B3 is thermodynamically more stable than phase B2. The peak at $2\theta \approx 19^\circ$, assignable to phase B1, increased before phases B2 and B3 simultaneously disappeared to form a single phase at 180°C. The peak characteristic to the (disordered) spinel phase at $2\theta \approx 31^\circ$ was unclear at around 200°C in this case. At 300°C the peak at $2\theta \approx 19^\circ$ for phase B4 nearly vanished and the rocksalt $Li_{1-z}Ni_zO$ phase with peaks at $2\theta \approx 37.5^\circ$ and 43.5° became distinct.

Sample B exhibited similar TG-DSC behavior to sample A, as shown in Fig. 11. The weight loss started at around 190°C. The exothermic peak at 200°C was less pronounced than that for sample A, probably due to the low stability of the corresponding spinel phase. A DSC dent at 220°C could result from the overlaid heat of the above exothermic reaction and endothermic oxygen evolution. The sample weight was nearly unchanged at temperatures above 500°C, and the final product at 700°C again had a rocksalt structure with a cubic lattice parameter of $a = 8.36$ (4.18×2) Å. There was a weight loss of 17.3%, which is again close to the expected value of 16.9%.

The changes in sample B up to 180°C were again irreversible, and we isolated the product heated at 180°C, namely,

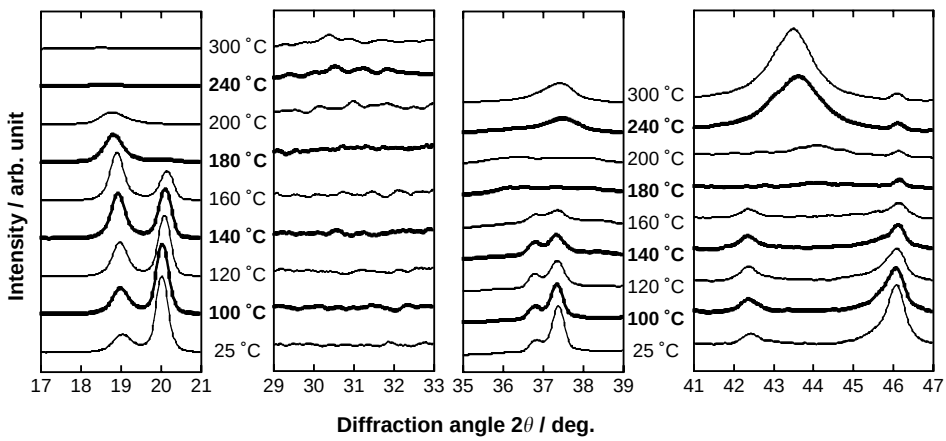

FIG. 10. XRD patterns of sample B heated at temperatures between 25 and 300°C. The intensity was varied for different angle regions for clarity. The peak at 46.2° corresponds to the 200 peak of platinum used as the sample holder.

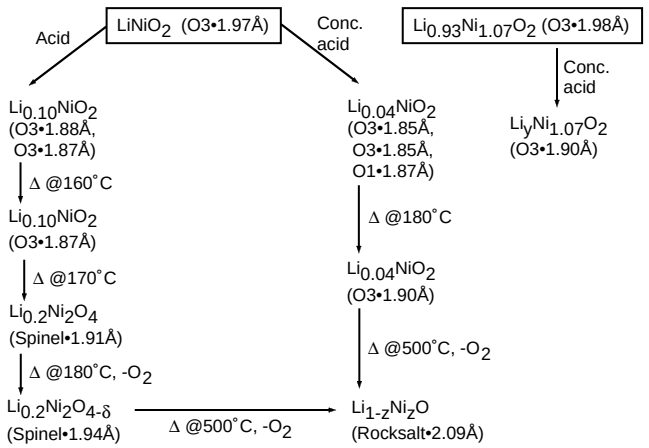

FIG. 12. Reaction scheme of lithium nickelate. O1 and O3 in the parentheses denote the NiO_2 stacking manner of the cadmium iodide and chloride structures, respectively. The length in Å corresponds to the Ni–O distance.

sample G with phase B4 (see Table 1). The XRD peaks were only poorly defined. The derived hexagonal lattice parameters were $a = 2.92$ Å and $c = 14.2$ Å. The c/a ratio was close to $\sqrt{24}$ (4.90), indicating that the pristine two-dimensional nature of sample B was degraded at 180°C and that this material can belong to the cubic system with a lattice parameter of 8.2–8.3 Å. We think that the sliding of the NiO_2 units, caused by phase B3 formation, brought about the loss of crystallinity followed by the degradation of the pristine layered material.

4. CONCLUSIONS

Treating $LiNiO_2$ with sulfuric acid results in highly delithiated compounds, Li_xNiO_2. Thus obtained $Li_{0.10}NiO_2$ consists of two phases with NiO_2 stacking similar to cadmium chloride (O3-type). The more delithiated nickelate $Li_{0.04}NiO_2$ additionally contains an NiO_2 phase with a cadmium iodide structure (O1-type). In an NiO_2 composition with no lithium in the interlayer, the O1-type seems to be thermodynamically more stable than the O3-type. Therefore, one of the O3-type phases in $Li_{0.04}NiO_2$ probably changes into the O1-type phase as a result of the NiO_2 sheet sliding. Such sliding is hindered by Ni^{2+} contained in $Li_{0.93}Ni_{1.07}O_2$. The two phases contained in $Li_{0.10}NiO_2$ combine at around 160–170°C to form a single O3-type phase, which is further transformed to spinel phase before decomposing into a rocksalt phase $Li_{1/11}Ni_{10/11}O$ at above 500°C. Two new polymorhs with the nominal composition of $Li_{0.10}NiO_2$ are obtained by heating the pristine $Li_{0.10}NiO_2$ (obtained by the acid treatment). One of them has a single O3-type phase and the other a spinel-related phase. Our thermal analysis of $Li_{0.04}NiO_2$ indicated that the intermediate phases at around 180°C have low crystallinity because of the sliding NiO_2 sheet, but the final product at above 500°C is again the rocksalt phase.

Figure 12 summarizes the reaction scheme that we obtained in this study. This figure shows that various kinds of "nickel dioxide" are obtained using acid treatment and low temperature heating, demonstrating the usefulness of "soft chemical" methods for synthesizing metastable compounds. Another interesting matter is that these polymorphs can exhibit varied characteristics. For example, we have found that their electrochemical behavior upon lithium insertion differs greatly, as we will report elsewhere. Examining these polymorphs will enable us to clarify the relationship between structure and other characteristics, and to design new functional materials.

ACKNOWLEDGMENTS

The authors express their gratitude to Ichiro Yamada and Kazuhiko Komatsu for their encouragement during the course of this research. The authors are grateful to Noriko Kurusu and Ryuichi Nishio for their excellent technical support. The authors also thank Miho Kanazawa for supporting the XPS measurement.

REFERENCES

1. W. Levason and C. A. McAuliffe, *Coord. Chem. Rev.* **12,** 151 (1974).
2. T. Ohzuku, A. Ueda, and M. Nagayama, *J. Electrochem. Soc.* **140,** 1862 (1993).
3. W. Li, J. N. Reimers, and J. R. Dahn, *Solid State Ionics* **67,** 123 (1993).
4. H. Arai, S. Okada, H. Ohtsuka, M. Ichimura, and J. Yamaki, *Solid State Ionics* **80,** 261 (1995).
5. G. G. Amatucci, J. M. Tarascon, and L. C. Klein, *J. Electrochem. Soc.* **143,** 1114 (1996).
6. H. Arai, S. Okada, Y. Sakurai, and J. Yamaki, *Solid State Ionics* **95,** 275 (1997).
7. L. Seguin, G. Amatucci, M. Anne, Y. Chabre, P. Strobel, J. M. Tarascon, and G. Vaughan, *J. Power Sources* **81–82,** 604 (1999).
8. J. M. Tarascon, G. Vaughan, Y. Chabre, L. Seguin, M. Anne, P. Strobel, and G. Amatucci, *J. Solid State Chem.* **147,** 410 (1999), doi: 10.1006/jssc.1999.8465.
9. L. Croguennec, C. Pouillerie, and C. Delmas, *J. Electrochem. Soc.* **147,** 1314 (2000).
10. L. Croguennec, C. Pouillerie, and C. Delmas, *Solid State Ionics* **135,** 259 (2000).
11. A. N. Mansour, X. Q. Yang, X. Sun, J. McBreen, L. Croguennec, and C. Delmas, *J. Electrochem. Soc.* **147,** 2104 (2000).
12. L. Croguennec, C. Pouillerie, A. N. Mansour, and C. Delmas, *J. Mater. Chem.* **11,** 131 (2001).
13. J. C. Hunter, *J. Solid State Chem.* **39,** 142 (1981).
14. J. Morales, C. Pérez-Vicente, and J. L. Tirado, *Mater. Res. Bull.* **25,** 623 (1990).
15. J. Morales, C. Pérez-Vicente, and J. L. Tirado, *J. Therm. Anal.* **38,** 295 (1992).
16. E. Zhecheva and R. Stoyanova, *Mater. Sci. Forum.* **152–153,** 259 (1994).
17. R. Alcántara, J. Morales, J. L. Tirado, R. Stoyanova, and E. Zhecheva, *J. Electrochem. Soc.* **142,** 3997 (1995).
18. G. Dutta, A. Manthiram, J. B. Goodenough, and J. C. Grenier, *J. Solid State Chem.* **96,** 123 (1992).
19. H. Arai and Y. Sakurai, *Denki Kagaku* **66,** 1206 (1998).

20. H. Arai and Y. Sakurai, *J. Power Sources* **81–82,** 401 (1999).
21. H. Arai and Y. Sakurai, *Mater. Res. Soc. Symp. Proc.* **575,** 3 (2000).
22. F. Izumi, *in* "The Rietveld Method" (R. A. Young, Ed.), p. 236. Oxford Univ. Press, Oxford 1993.
23. F. Izumi and T. Ikeda, *Mater. Sci. Forum*, **321–324,** 198 (2000).
24. R. A. Young, *in* "The Rietveld Method" (R. A. Young, Ed.), p. 22. Oxford Univ. Press, Oxford 1993.
25. R. D. Shannon, *Acta Crystallogr. Sect. A*: *Found. Crystallogr.* **32,** 751 (1976).
26. A. N. Mansour, *Surf. Sci. Spectra* **3,** 231 (1996).
27. A. N. Mansour and C. A. Melendres, *Surf. Sci. Spectra* **3,** 271 (1996).
28. A. N. Mansour and C. A. Melendres, *Surf. Sci. Spectra* **3,** 287 (1996).
29. M. Yoshimura, K.-S. Han, and S. Tsurimoto, *Solid State Ionics* **106,** 39 (1998).
30. M. Schulze, R. Reissner, M. Korenz, U. Radke, and W. Schnurnberger, *Electrochim. Acta* **44,** 3969 (1999).
31. F. Ronci, B. Scrosati, V. R. Albertini, and P. Perfetti, *J. Phys. Chem. B* **105,** 754 (2001).
32. J. R. Dahn, E. W. Fuller, M. Obrovac, and U. von Sacken, *Solid State Ionics* **69,** 265 (1994).
33. T. Ohzuku, A. Ueda, and M. Kouguchi, *J. Electrochem. Soc.*, **142,** 4033 (1995).
34. D. Wainwright, *J. Power Sources* **54,** 192 (1995).
35. H. Arai, S. Okada, Y. Sakurai, and J. Yamaki, *J. Electrochem. Soc.* **144,** 3117 (1997).
36. K. Yamaura, M. Ami, and K. Sekai, *in* "Meeting Abstract of the 1997 Joint International Meeting of The Electrochemical Society and The International Society of Electrochemistry," Vol. 97–2, p.128, Paris (1997).
37. H. Arai, S. Okada, Y. Sakurai, and J. Yamaki, *Solid State Ionics* **109,** 295 (1998).
38. M. G. S. R. Thomas, W. I. F. David, and J. B. Goodenough, *Mater. Res. Bull.* **20,** 1137 (1985).
39. R. Kanno, H. Kubo, Y. Kawamoto, T. Kamiyama, F. Izumi, Y. Takeda, and M. Takano, *J. Solid State Chem.* **110,** 216 (1994).